# Experimental investigation of tandem arrangement of two inverted flags in the wake of a cylinder

Author

Danish Ahmad

00000171022

Supervisor

Dr Zafar Abbas Bangash

DEPARTMENT OF MECHANICAL ENGINEERING

COLLEGE OF ELECTRICAL & MECHANICAL ENGINEERING

NATIONAL UNIVERSITY OF SCIENCES AND TECHNOLOGY

ISLAMABAD

OCT, 2019

# Experimental investigation of tandem arrangement of two inverted flags in the wake of a cylinder

Author

Danish Ahmad

00000171022

A thesis submitted in partial fulfillment of the requirements for the degree of

MS Mechanical Engineering

Thesis Supervisor:

Dr Zafar Abbas Bangash

Thesis Supervisor's Signature: _____

DEPARTMENT OF MECHANICAL ENGINEERING

COLLEGE OF ELECTRICAL & MECHANICAL ENGINEERING

NATIONAL UNIVERSITY OF SCIENCES AND TECHNOLOGY,

ISLAMABAD

OCT, 2019

# Declaration

I certify that this research work titled "*Experimental investigation of tandem arrangement of two inverted flags in the wake of a cylinder"* is my own work. The work has not been presented elsewhere for assessment. The material that has been used from other sources it has been properly acknowledged / referred.

Signature of Student

Danish Ahmad

00000171022

# Language Correctness Certificate

This thesis has been read by an English expert and is free of typing, syntax, semantic, grammatical and spelling mistakes. Thesis is also according to the format given by the university.

Signature of Student

Danish Ahmad

00000171022

Signature of Supervisor

# Copyright Statement

# Acknowledgements

I am thankful to my Creator Allah Subhana-Watala to have guided me throughout this work at every step and for every new thought which Your setup in my mind to improve it. Indeed, I could have done nothing without Your priceless help and guidance. Whosoever helped me throughout the course of my thesis, whether my parents or any other individual was Your will, so indeed none be worthy of praise but You.

I am profusely thankful to my beloved parents who raised me when I was not capable of walking and continued to support me throughout in every department of my life.

I would also like to express special thanks to my supervisor Dr. Zafar Abbas Bangash for his help throughout my thesis and also for Heat and Mass Transfer course which he has taught me. I can safely say that I haven't learned any other engineering subject in such depth than the ones which he has taught.

I would also like to pay special thanks to Dr. Emad Uddin for his tremendous support and cooperation. Each time I got stuck in something, he came up with the solution. Without his help I wouldn’t have been able to complete my thesis. I appreciate his patience and guidance throughout the whole thesis.

I would also like to thank Dr Zaib Ali and Dr. Ali Zaidi for being on my thesis guidance and evaluation committee. I am also thankful to Muhammad Umair and Rafay for their support and cooperation.

Finally, I would like to express my gratitude to all the individuals who have rendered valuable assistance to my study.

*Dedicated to my exceptional parents and adored siblings whose tremendous support and cooperation led me to this wonderful accomplishment*

# Abstract

Analysis of different arrangements of the piezoelectric flexible bodies are of keen interest due to their performance variation. Inverted flags (leading free and trailing clamped end) are currently trending because of their greater amplitudes of oscillation and ambient friendly nature (i.e. they can flap at low flow speed also). Varying flexural rigidities and studying their effects have also been of great interest for the researchers. Here we have observed the tandem arrangement of inverted flags and investigated the effects of increasing flexural rigidity "$\gamma$", stream wise gap between them "Gx/L" and velocity of the flow "V" in water tunnel. Voltages produced "$V_{rms}$", flapping frequency of the rear flag decreased by increasing the rigidity whereas the amplitude over length of the flag "A/L" was almost unchanged. A/L and frequency were affected by the increase of velocity. Also varying stream wise gap "Gx/L" had significant influence on the performance of the rear flag. Stream wise gap "Gx/L" between 1~2 showed greater performance of the flag as all the three parameters were at their peaks. Below Gx/L=1, rear flag flaps with negligible amplitudes and flapping frequencies which led to the least values of $V_{rms}$ generated. Parameters of the upstream flag were not observed because of their minute values due to inverted drafting phenomenon. However, amplitudes of both the flags were compared for the observed purpose of that phenomenon which agreed well. Furthermore, the rear got deflected even at very low flow velocities due to which leading flag did not experience much flapping.

**Key Words:** *Inverted flags, Tandem arrangement, Flexural rigidity*

# Table of Contents

# List of Figures

# List of Tables

# CHAPTER 1: INTRODUCTION

For the evaluation of performance of different arrangements of piezoelectric flags, water tunnel is used. Main difference between the water tunnel and wind tunnel setup is of the medium used in the tunnel i.e. water and air respectively. Water tunnel is preferred when flow visualization is required. For the said purpose Particle Image Velocimeter (PIV) is used. Also, for the calculation of lift and drag force, water tunnel is the best choice.

## 1.1. Background

Renewable energy sources are used for centuries for the generation of electric power. The nonpolluting nature and very low capital cost makes them the best choice. According to the article published by Climate Council, developed country like Sweden is trying to make the country "fossil fuels free power generation" by 2040. Pakistan also is on the path towards consuming more renewable sources and many projects from high cost dams to the small scale projects are in different phases of completion. In recent years, piezoelectric materials are gaining attention of the researchers for the generation of small scale electric power. Many experimental and computational work has been done on the optimization of the system.

## 1.2. Work Scope

Objective of the experimentation is to evaluate the performance of two inverted flags in tandem arrangement. Main aim is investigate the effect of varying flexural rigidity "γ", stream wise gap between them "Gx/L" and flow velocity "v" on the root mean square voltages "$V_{rms}$" generation, flapping frequency and amplitude over length "A/L" of the rear flag". For this purpose, 3 different flexural rigidities have been selected i.e. 0.001,0.0015 and 0.002 N.m. Range of the stream wise gap

between the flags has been selected between 0.5~2.5 with a step size of 0.5. Flow velocity has been varied between 0.17~0.3 m/s.

## 1.3.Conventional Flag

A flag whose leading edge is fixed, and trailing edge is free to flap is the conventional arrangement of the flag. The flow of the fluid after passing the clamp of the flag approaches the free trailing edge and compels it to flap. Conventional flags exhibit three modes: a stretched straight mode, a fluttering mode, and a periodic flutter mode. There isn't any deflection mode which happens only in inverted configuration of flexible flag. The amplitude "A/L" of this configuration of flag never exceeds 0.5[29].

## 1.4.Inverted Flag

When the trailing edge of a flag is fixed while the leading edge can flap freely, then this configuration of flexible body is known as inverted arrangement of flag represented in figure 1.

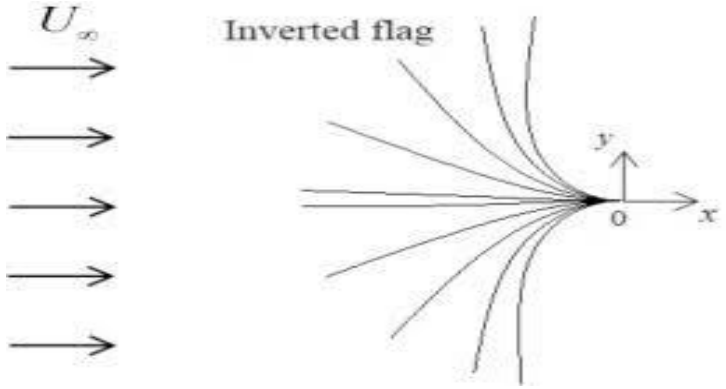


**Figure 1** Schematic of a flag in inverted configuration

Many researchers have showed their interest in working on inverted flags due to their greater amplitudes than that of the conventional configuration of flag. Orrego recently in 2017 worked on energy harvesting with an inverted flag. He presented three modes of inverted flag

dependent upon the bending stiffness "$K_B$". When $K_B$=0.4 the flag remains straight. As the value of bending stiffness decreases to 0.3, the flag starts to flap with large amplitude periodic flapping until it decreases to 0.1. Below this value of $K_B$ the flag deflects to a side with almost zero flapping frequency. All these modes of inverted flag are shown in figure 2.

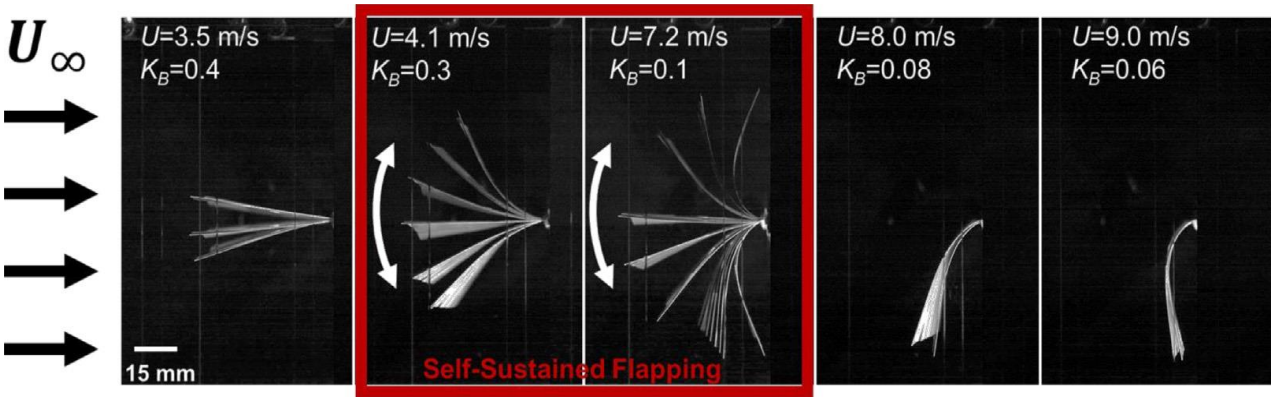


**Figure 2** Flapping modes of an inverted flag depending upon bending stiffness.[23]

He stated that the amplitude over length ratio "A/L" of an inverted flag can reach up to 1.7 whereas "A/L" of a conventional flag can be around 0.8[23]. Also this configuration of flag is ambient friendly i.e. energy can be harvested at very low flow velocities (in our case the range for the flow velocity is 0.17~0.3 m/s). There is a phenomenon of deflection in this configuration of flexible body. At higher flow velocity the flag gets deflected to a side with negligible flapping frequency. The flag stays at deflected until the flow is stopped.

## 1.5. Tandem Arrangement of Inverted Flags

When multiple inverted flags are arranged in such a way that they are one behind another then this arrangement of the flags is known as tandem arrangement of inverted flags as shown in figure 3. Researchers are working on to find out the optimal stream wise gap between the flags to acquire maximum energy out of them. There is a phenomenon of inverted drafting which occurs only in flexible bodies when they are aligned across the flow. The downstream flexible body experiences more drag and flaps with greater amplitude than the upstream flag which is

contrary to the conventional drafting which occurs in rigid bodies. Fish schooling is an example of this phenomenon.

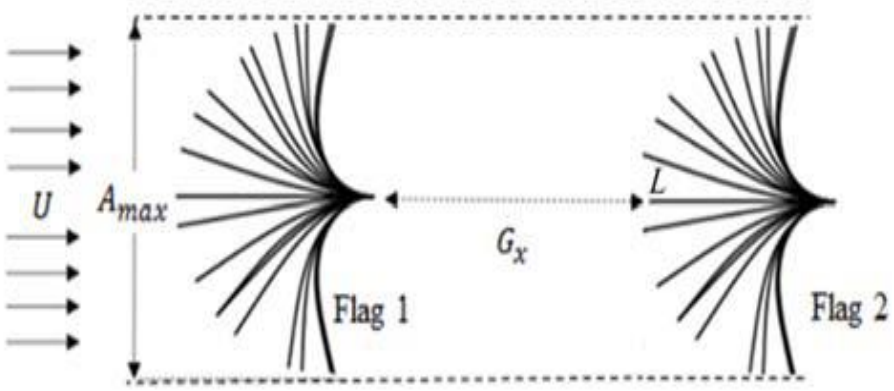


**Figure 3** Tandem arrangement of two inverted flags [25]

# CHAPTER 2: LITERATURE REVIEW

## 2.1.Fundamental Concept of Vortex Induced Vibration (VIV)

Mobassher in 2012 discussed the basic concepts of Vortex Induced Vibration along with its parameters. The vortices are generated alternatively from one side to the other and in result of these vortices at the back of the object, unsteady oscillating pressures are generated which cause the object to vibrate [1].

## 2.2.Vortex Shedding at Different Reynolds Numbers

No vortices are generated at Reynolds Number equals to or less than 5. Nishioka in 1978 did experimental investigation of wake behavior of downstream of a cylinder at Reynolds Numbers between 20 to 150. Low speed wind tunnel was used for this purpose with a range of flow speed of 10 to 100 cm/s. The very first time the vortices are generated in this Reynolds numbers range and their lengths get increases as the Reynolds number increases. The length of the vortices can reach up till 3 times of the diameter of the cylinder at Reynolds Number 45. [2]. Effects on the vortices by increasing Reynolds number beyond 45 has been studied by Huerre and Monkewitz in 1990 and they proposed that the stability of the wake is disturbed [3].

Friehe in 1980 carried an experiment to observe the shedding frequency and velocity of the free stream passing by cylinders of length to diameter ratio of greater than 150. The range of Reynolds number was from 50 to 175. Results show that breakage of one of the vortices happened in this range [4].

Anatol Roshko in 1954 selected Reynolds number ranges from 40 to 10000 and using wind tunnel, analyzed the wake dynamics behind a circular cylinders of diameter ranges from 0.0235 to 0.635 cm. On the basis of the flow dynamics, two ranges were set. Below Re=150 was a

stable range where the flow was laminar and viscous configuration was dominant. Beyond 150, the range was a transitional range where turbulence got involved. Only the vortices in the wake region are turbulent. The boundary layer is still laminar [5].

Roshko in 1961 observed an increase in drag coefficient of over a large cylinder placed in wind tunnel for the experimentation purpose. The range of Reynolds numbers selected was 106 to 107. Results show the drag coefficient increment from its super critical value and attaining 0.7 at Reynolds number 3.5*106. Also vortex shedding started to occur again with complete turbulence of vortices as well as the boundary layer [6]. Nickerson and Dias in 1981 proposed by the help of an experimentation that vortex shedding can occur up till Reynolds number 1011 [7].

## 2.3. Vortex Shedding Across Single Cylinder

Griffin and Ramberg in 1975 investigated the wake formation downstream of a rigid cylinder. Results of their investigation showed that when the cylinder vibrates with a frequency approximately equal to the frequency of vortices being shed, vortices are shed with a great strength [14]. Bishop and Hassan in 1964 presented findings of their experiment and showed that, the cylinder experiences more drag force [15].

## 2.4. Vortex Shedding Across Multiple Cylinders

Cylinder near a plane and multiple cylinders' arrangements are also been observed by researchers to see their hydrodynamics and vortices formation and shedding of these vortices. Torum and Anand in 1985 proposed that the vortex shedding can occur if the gap between the cylinder and the surface remains greater than 0.5 diameter [8]. Tsahalis in 1984 used wave tank for observing the effect of the gap distance between the plane and a flexible pipe. Results shows great response of the amplitude as well as of the frequency to the variation in gap distance [9].

Bearman in 1978 did experimentation in a wind tunnel to find out the effects of varying height of the cylinder from a plane boundary. Results show that a gap distance of 0.3 diameter is needed if suppression of vortex shedding is to be avoided [10]. Buresti and Lanciotti in 1979 performed an experiment using a wind tunnel. The Reynolds number was set between 0.85*105 and 3*105. Results show that the vortex shedding mechanism stayed unchanged up till distance to diameter ratio is greater than 0.4 [11].

Kiya in 1980 did an experiment to study the frequency of vortex shedding of two circular cylinders in staggered arrangement. The Reynolds Number kept was 1.58*104. Results show that vortex shedding persists downstream of both the cylinders if the gap distance is kept greater than 0.4 diameter. Below this gap, each of the cylinder will have a behavior of single object [12].

## 2.5. Universal Strouhal Number

Sarpkaya in 1979 proposed a concept of Universal Strouhal Number. According to his findings, bluff body of any shape can have a Strouhal Number of approximately 0.2 for a wide range of Reynolds Number if the character dimension “D” is taken as the width of the separation [13]

Stansby in 1976 investigated the frequency shedding phenomenon around circular cylinders and concluded that a sudden alteration of 180 degree occurs between the vortex shedding and vibration of the cylinder as frequency of both the vibration matches [16]. Williamson in 1988 presented his findings by stating that the vortices start to split up at a point where the amplitude of the oscillation goes beyond almost one and half of the cylinder diameter [17].

Blevins in his book on Flow Induced Vibrations (Section 3.3; Chap 3) stated that average value of Coefficient of Drag is the function of

amplitude of the oscillation. There is direct relation between the drag and the amplitude of vibration. [18]. Bearman in 1982 did experimental study on square cross-section cylinders and concluded that the drag force increases as the oscillation amplitude increases [19].

## 2.6. Vortex Shedding Across a Flat Plate

Teimourian in 2017 reviewed numerically the vortex shedding downstream of a flat plate having different arrangements consisting single plate, tandem and side by side arrangements. Most of the literature has been covered on single plate. Among the different turbulent models, direct numerical simulation (DNS) is mostly used by researchers [20]. Bently and Mudd investigated the shedding effect and the effects of gap distance for various bluff bodies. He concluded that bluff bodies that are closely spaced in tandem arrangement have the same behavior of a single body. As the gap is increased, vortices start to separate from the bluff body and the effects of these vortices start to appear [21].

## 2.7. Flapping Dynamics of a Single Inverted flag

Daegyoum Kim experimentally explained the dynamics of an inverted flag in an open-loop wind tunnel. The cross section of the tunnel was 1.2*1.2 m with the range of velocity produced from 2.2 to 8.5 m/s. Three modes of the flag were observed at different bending stiffness. The flag was in straight mode at bending stiffness less than or equal to 0.3. Between 0.3 and 0.1 values of the bending stiffness, flag was presenting the flapping mode. Beyond the value of 0.1, the flag was completely deflected with negligible power generating capacity[22].

## 2.8.Energy Harvesting of a Single Flag

Orrego in 2017 harvested peak electric power of 5 mW/cm3 in an ambient wind condition of almost 9 m/s using an inverted flag with maximum amplitude of approximately A/L equal to 1.8. The peak was found to be around $K_B$ equal to 0.1. Also a self-aligning mechanism was introduced to adjust according to the wind direction. Endorsing Kim's findings, the flag was in self sustained flapping mode when bending stiffness value was between 0.1 and 0.3. A temperature sensor was powered 20 times more than the conventional arrangement of a piezoelectric flag [23].

## 2.9.Two Flags in Tandem Arrangement

Sohae Kim in 2010 performed numerical simulation of 2 tandem flags in normal configuration to investigate the constructive and destructive mode of interaction of the vortices generated by the flags. The drag force increases in constructive mode and vice versa. Simulation was performed to figure out the effect of stream wise and span wise gap distances on the drag force at Reynolds number greater than or equal to 200 and less than or equal to 400. Results of the simulation show that the amplitudes and the drag forces on the both flags are higher than of the single flag as the gap distance goes higher than 1 at Reynolds number equal to 200. At Reynolds number 400 and between the range of 1.05 and 1.15 stream wise gap distance, drag force as well as the amplitude of the rear flag decreased sharply. [24].

S. Mazharmanesh in December 2018 used an immersed boundary method to analyze the performance of two inverted tandem flags. The simulation was run at Reynolds number of 100 and the stream wise gap distance was varied from 1 to 3.2. The computational domain of 42L*42L rectangular box with 2.1*105 mesh size was used for this purpose. Two parameters are introduced here as piezo mechanical coupling parameter "@" and piezoelectric tuning parameter "$\beta$". Time average of power

coefficient “Cp” has an optimal value at Gx/L=1.8 and @=0.5 and $\beta$ =1.5 [25].

Huang in 2017 numerically investigated performance of inverted eels in a tandem arrangement. Direct Numerical Simulation is used for the said purpose. Reynolds number is kept at 200. Results show that as the stream wise gap is increased, drag coefficient of the downstream flag increases until a limit comes beyond which both the flags behave like an isolated flag. Also gap less than 2 will lower the drag coefficient of the downstream flag than that of single flag [27].

## 2.10. Blockage Ratio

Choi in 1998 experimentally investigated blockage ratio of a square model wind tunnel. The cross section of the test section is 1*1 m with a maximum velocity of 17 m/s. Findings of his research is that blockage ratio can be allowed up to 10% with negligible effects on the experiments [26].

# CHAPTER 3: THEORETICAL STUDIES

## 3.1. Basic Definitions

### 3.1.1. Viscosity

Viscosity is the internal resistance between the two neighboring layers of flowing fluid.

### 3.1.2. Kinematic Viscosity

Kinematic viscosity is the dynamic viscosity per density of the fluid.

### 3.1.3. Blockage Ratio

It is defined as ratio of the area of the model perpendicular to the flow to the cross-section area of the test section. It should not cross 5% for better results.

### 3.1.4. Critical angle of attack

It is the angle of attack at which maximum lift coefficient can be attained. Below this angle, lift coefficient has direct relation with angle of attack. Mostly this angle is around 15 to 20 degree.

### 3.1.5. Stalling

When an aircraft exceeds its given critical angle of attack and is unable to produce the required lift for normal flight. The critical angle of attack is almost 15 degrees.

## 3.2.Basic Formulae

### 3.2.1. Bending Stiffness

It is defined as the opposition proposed by the structure to the bending deformation.

$$\mathrm{K}_b = \frac{Eh^3}{12(1-v^2)\rho_f U^2 L^3}$$

### 3.2.2. Mass Ratio

Mass ratio in fluid mechanics is the ratio of the mass of the substance to the mass of the fluid containing it.

$$M = \frac{\rho_h}{\rho_f L}$$

### 3.2.3. Reynolds Number

It is dimensionless number representing the ratio of the inertial force to the viscous force inside the fluid. Reynolds number differentiate between the laminar and turbulent flow.

$$Re = \frac{\rho UL}{\mu}$$

### 3.2.4. Froude Number

A dimensionless number defined as ratio of flow inertial force to the external or in specific gravitational force is known as Froude number.

$$F_r = \frac{U}{gl^{1/2}}$$

### 3.2.5. Strouhal Number

A non-dimensional number which is used to analyze the dynamics of unsteady fluid flow. It represents the relation between the vortex shedding frequency and the velocity of the fluid.

$$\mathrm{S} = \frac{\mathrm{fD}}{\mathrm{U}}$$

### 3.2.6. Vortex Shedding Frequency

Cycles of vortices shed per unit second is the vortex shedding frequency.

### 3.2.7. Aspect Ratio

Aspect ratio is defined as the width over the height of an object.

$$AR = \frac{W}{H}$$

## 3.3. Vortex Generation and Shedding

### 3.3.1. Vortex Generation

As fluid passes a solid object at low Reynolds Numbers I.e. Re<=5, the fluid follows the shape of the object all away around and passes smoothly. The streamlines of the fluid will have symmetric configuration around the body with oscillating high pressure at the front and back and low pressure at the top and bottom of the object placed in flow stream. As the Reynolds Number passes the barrier of 5, vortices start to form at the back of object. In case of the flapping flag, these vortices are formed alternatively from both side. They remain inside the wake behind the body until a certain number.

### 3.3.2. Vortex Shedding

Vortices start to break from the object as the Reynolds number approaches almost 100. Flapping of the flag propels the vortices and new vortices take place of the previous ones. In case of multiple flags in tandem or staggered arrangement, these vortices of the former flag interfere with the vortices of the rear flag constructively or destructively depending upon the stream wise and span wise gap between the two flags. The increment or decrement of the amplitude and drag force acting on the rear flag depends on whether the vortices are meeting constructively or destructively. Liehard in 1966 studied the vortex generation and shedding downstream of a cylinder at different Reynolds number represented in figure 4.

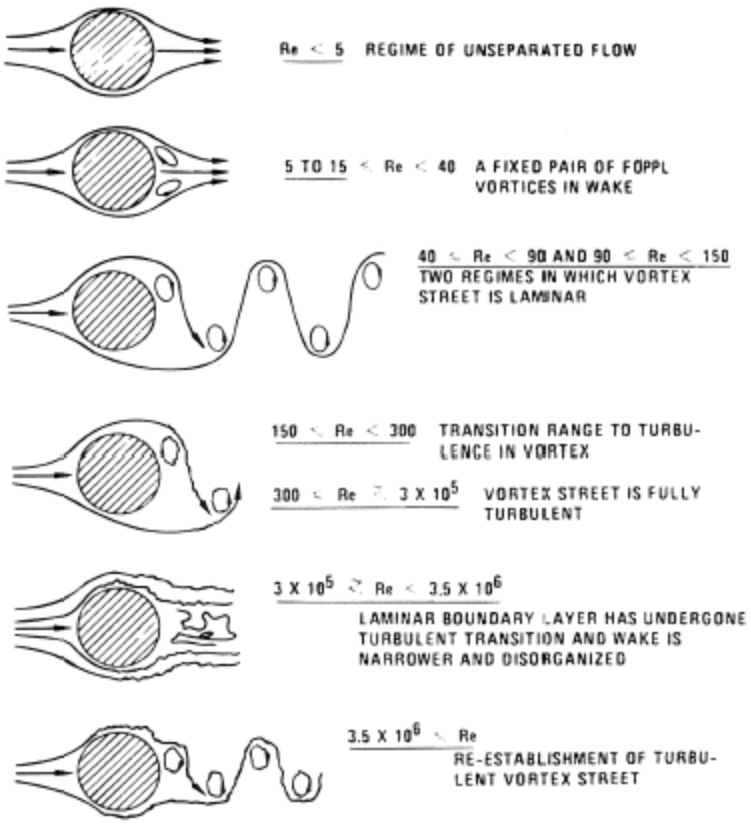


**Figure 4** Vortex Shedding behind a cylinder at different Reynolds Number[30]

## 3.4.Fluttering

### 3.4.1. Instability

If the oscillating fluid force tends to increase the vibration of the object, the structure is aerodynamically unstable and very large amplitude can result.

### 3.4.2. Fluttering

Torsion plunge instability of airfoil structures which is dynamic and static instability due to stalling is fluttering in airfoil structures. Fluttering occurs in stall region where the angle of attack exceeds the critical value of 15 degrees.

### 3.4.3. Galloping

One degree of freedom instability of bluff structure in civil engineering is known as galloping. For galloping, the value of reduced velocity should be less than 20 and the angle of attack less than 15 degrees.

## 3.5. Forces on the structure in the flowing fluid field

### 3.5.1. Drag Force

A force that acts in the opposite direction of any object moving with respect to a surrounding fluid is known as drag force. It opposes motion of the structure in the fluid field.

$F_D = 1/2 * (C_D * V^2 * A)$

### 3.5.2. Lift force

Force that is perpendicular in direction to the oncoming flow direction is known as lift force. It usually acts in the upward direction.

Lift coefficient "$C_L$" has direct relation with the angle of attack till it gets to the maximum. Beyond the critical angle of attack, the lift force starts to decrease again.

# CHAPTER 4: EXPERIMENTAL SETUP

Experimentation is carried out in a water tunnel placed at Hydraulics Lab Department of Mechanical Engineering NUST. The setup consists of a cylinder, two piezoelectric flags, a pump, a high frame rate camera, Data Acquisition System (DAQ) and a Light Emitting Diode (LED). Setup inside the tunnel (i.e. two piezoelectric flags in inverted configuration along with a circular cylinder) is represented in figure 5.

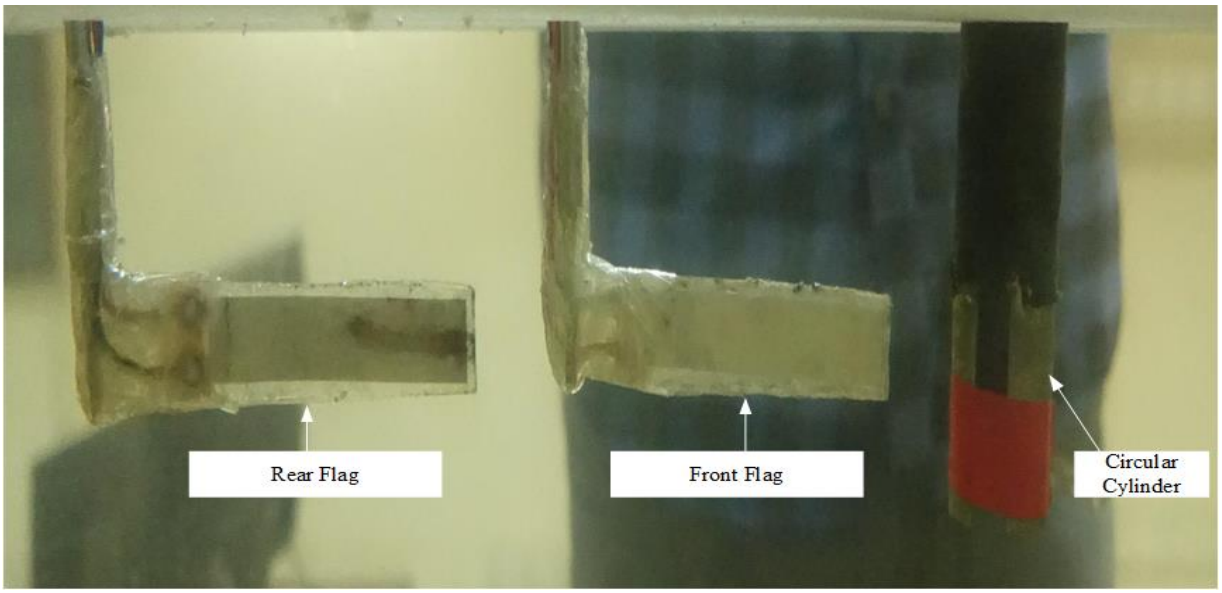


**Figure 5** Experimental Setup having 2 Flapping flags with an upstream bluff body (circular cylinder)

The whole setup is described in detail as follows.

## 4.1. Water Tunnel

The tunnel is placed in the lab with a square test section of length of 2000 mm and frontal area of 400 * 400 mm. Test section is made of acrylic with the thickness of 10mm. 8 honeycombs are placed upstream of the bluff body (cylinder) with the cell size of length to diameter ratio of 6 to 8. It channelizes the water flow and lowers the turbulence of the flowing water. Test section of the tunnel is shown in figure 6.

**Figure 6** Test section

## 4.2. Centrifugal Pump

A 1450 RPM centrifugal pump is used for the purpose of flowing water across the flags and cylinder. The frequency can be varied between 0 to 50 Hz with 10 Horse power. It can regulate the water speed up to 0.5 m/s. Figure 7 represents the pump used for our experimentation.

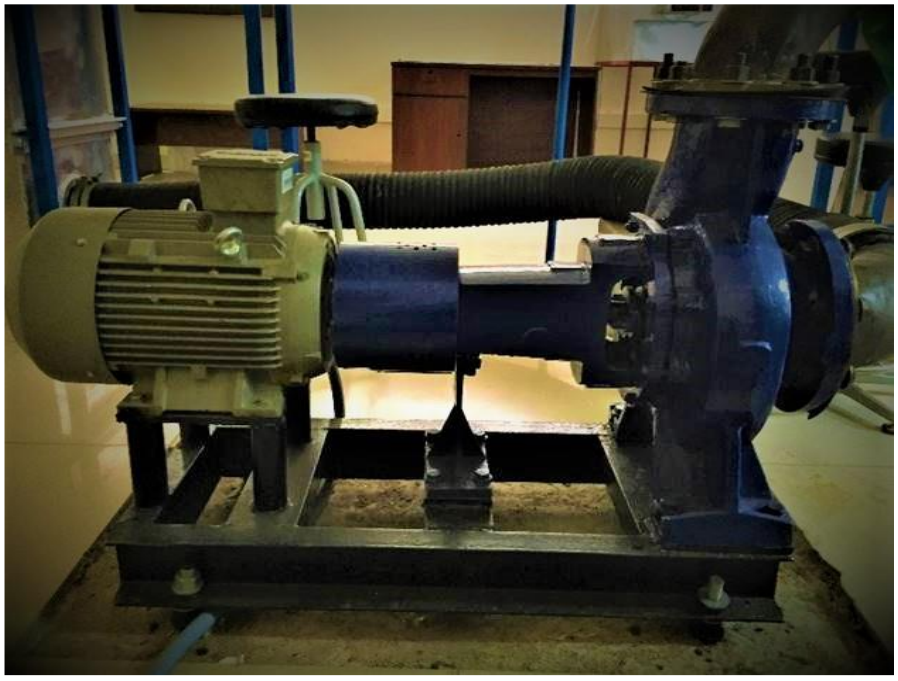

**Figure 7** Centrifugal Pump

## 4.3.Cylinder

A cylinder of 25 mm is placed upstream of the front flag for the purpose of vortex generation. The cylinder is made of stainless steel. It is placed at constant distance to diameter "S/D" ratio of 2 upstream of the front flag.

## 4.4.Piezoelectric Flags

The flags for the voltages generation purpose are made of Polyvinylidene Difluoride (PVDF) of 62mm length. The flags are 40µm and the laminated sheets used for the later cases are 60µm thick, Flexural rigidity of the flags vary between 0.001 N.m to 0.002 N.m. A single piezoelectric flag is shown in figure 8.


**Figure 8** Piezoelectric flag

All the mechanical and electrical properties of flags used in this experimentation has been given in table 1.

**Table 1** Mechanical and Electrical properties of the piezoelectric flags used.

| Symbol | Parameter | | PVDF | Units |
|---|---|---|---|---|
| t | Thickness | | 9, 28, 52, 110 | µm (micron, $10^{-6}$ ) |
| $d_{31}$ | Piezo Strain Constant | | 23 | $10^{-12}$ |
| $d_{33}$ | | | -33 | |
| $g_{31}$ | Piezo Stress constant | | 216 | $10^{-3}$ |
| $g_{33}$ | | | -330 | |
| $k_{31}$ | Electromechanical | | 12% | |
| $k_t$ | Coupling Factor | | 14% | |
| C | Capacitance | | .com/.,mb380 for 28ìm | pF/cm$^{2,}$ @ 1KHz |
| Y | Young's Modulus | | 2-4 | $10^9$ N/m$^2$ |
| $V_0$ | Speed of Sound | stretch: | 1.5 | |
| | | thickness: | 2.2 | $10^3$ m/s |
| p | Pyroelectric Coefficient | | 30 | $10^{-6}$ C/m$^2$ °K |
| å | Permittivity | | 106-113 | $10^{-12}$ F/m |
| å/å $_0$ | Relative Permittivity | | 12-13 | |
| $\rho_m$ | Mass Density | | 1.78 | $10^3$kg/m |
| $\rho_e$ | Volume Resistivity | | >$10^{13}$ | Ohm meters |
| $R_\square$ | Surface Metallization Resistivity | | <3.0 | Ohms/square for NiCu |
| $R_\square$ | | | 0.1 | Ohms/square for Ag Ink |
| tan ä$_e$ | Loss Tangent | | 0.02 | @ 1KHz |
| | Yield Strength | | 45-55 | $10^6$ N/m$^2$ (stretch axis) |
| | Temperature Range | | -40 to 80...100 | °C |
| | Water Absorption | | <0.02 | % $H_2O$ |
| | Maximum Operating Voltage | | 750 (30) | V/mil (V/µm), DC, @ 25°C |

| | | |
|---|---|---|
| Breakdown Voltage | 2000 (80) | V/mil (V/µm), DC, @ 25°C |

One of the latest advances in piezo electric polymer technology is piezoelectric cable. Power output is proportional to the strain on the cable. The long, thin piezo electric insulation layer provides relatively low output resistance (600 pF / m), which is unusual for a piezo electric device. The dynamic range of the cable is large (> 200 dB). It detects low-amplitude vibrations due to rain or cold, while responding linearly to the impact of heavy vehicles. Cables withstand pressure of 100 MPa. Normal operating temperature is -40 to 125 ° C Table 2 shows the characteristics of the piezo cable used in this experiment.

**Table 2** Properties of the piezo cable

| **Parameter** | **Units** | **Value** |
|---|---|---|
| Capacitance @ 1KHz | pF/m | 600 |
| Tensile Strength | MPa | 60 |
| Young's Modulus | GPa | 2.3 |
| Density | $kg/m^3$ | 1890 |
| Acoustic Impedance | MRayl | 4.0 |
| Relative Permittivity | @1KHz | 9 |
| tan $ä_e$ | @1KHz | 0.017 |
| Hydrostatic Piezo Coefficient | pC/N | 15 |
| Longitudinal Piezo Coefficient | Vm/N | $250 \times 10^{-3}$ |
| Hydrostatic Piezo Coefficient | Vm/N | $150 \times 10^{-3}$ |
| Electromechanical Coupling | % | 20 |
| Energy Output | mJ/Strain (%) | 10 |
| Voltage Output | kV/Strain (%) | 5 |

## 4.5.A high Frame Rate Camera

Sony cyber shot DSC-RX100 IV camera is used for the recording purpose. Its frame rate ranges between 30~1000 frames per second (Fps) with the resolution of 20.10 Megapixels. For our experimentation, the frame rate was kept 50Fps. Images were analyzed using image processing technique in MATLAB to determine the tail positioning of a flag in order to calculate peak to peak amplitude (A/L) and to superimpose the view of flag. (flapping envelope). Figure 9 represents the camera used for experimentation.


**Figure 9** A high frame rate camera

## 4.6.Data Acquisition System

Voltages generated $V_{rms}$ by the rear flag were measured using Data Acquisition System (DAQ Module in NI lab view) as shown in figure 10. The sample rate of measuring voltages was 50 with the number of sample to read =50. This means it measured the 50 samples of voltages in one second. After acquiring data from DAQ assistant, it was passed to the indicator where it read in LabVIEW and displayed as a number of charts for further processing (stored/analyzed).


**Figure 10** Data Acquisition System

## 4.7.Light Emitting Diode (LED):

A light emitting diode was used while recording the video. It was for a purpose recording better quality of video which was processed later using Image Processing tools in MATLAB and extracted frames and superimposed images of envelopes of the flag. Figure 11 represents the LED used for our experimentation.

**Figure 11** Light Emitting Diode (LED)

# CHAPTER 5: RESULTS

We experimentally observed the flapping dynamics of tandem inverted arrangement of two flags at three different flexural rigidities "$\gamma$" i.e. 0.001~0.002 N.m with a step size of 0.0005. The front flag was kept at stream wise gap "S/D=2" for all the experimentation due to the fact that the single inverted flag had traced maximum distance between the two extremes downstream of a bluff body. The stream wise gap "Gx/L" between the front and rear flag was varied between 0.5~2.5 with a step size of 0.5. Schematic of the setup inside the tunnel (i.e. a cylinder and two flapping flags) is represented in figure 12.

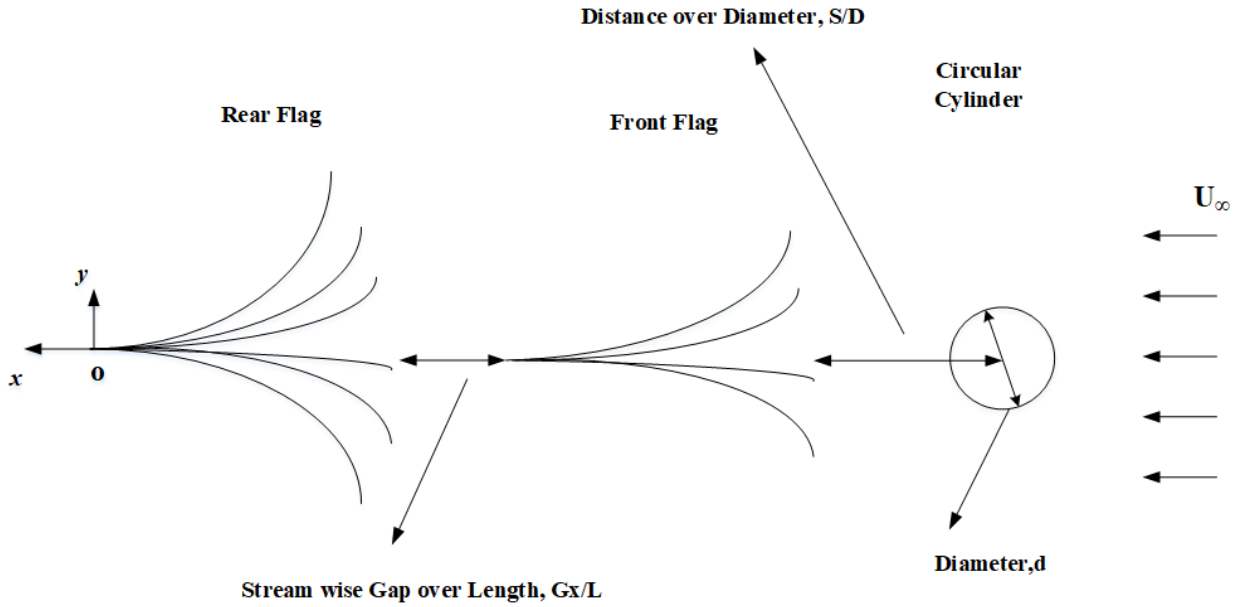


**Figure 12** Schematic of the setup (Top View)

The range of the flow velocity was between 0.17~0.3 m/s. Based on flexural rigidity we had 3 different cases with each case comprises of 36 configurations of stream wise gaps and flow velocities. Diameter of the bluff body (circular cylinder) was 25mm to avoid the effect of blockage ratio. Blockage ratio "D/H" for our experimentation was 6.25% which is in an

allowable range. After the experimentation carried out, voltages produced "$V_{rms}$", flapping frequency and the amplitude "A/L" of the rear flag were obtained by processing the data.

## 5.1. Case 1 "Maximum Values" (Flexural Rigidity=0.001 N.m)

In this case the flexural rigidity of the both flags were 0.001 N.m. The flow velocity at the start of the experimentation was 0.17 m/s at a stream wise gap "Gx/L" of 0.5. The flags started to flap with the minimum amplitude. Upstream flag flapped with comparatively lesser amplitude due to the inverted drafting phenomenon. Inverted drafting is a phenomenon found in flexible bodies where the downstream body (flag in our case) experiences higher drag than the upstream body which results in greater peak to peak amplitude of the rear body [28]. So flapping of the rear flag is of main consideration. Surface plots of the voltages produced "$V_{rms}$", flapping frequency and the amplitude "A/L" of the rear flag are presented in figure 13a, b and c respectively.

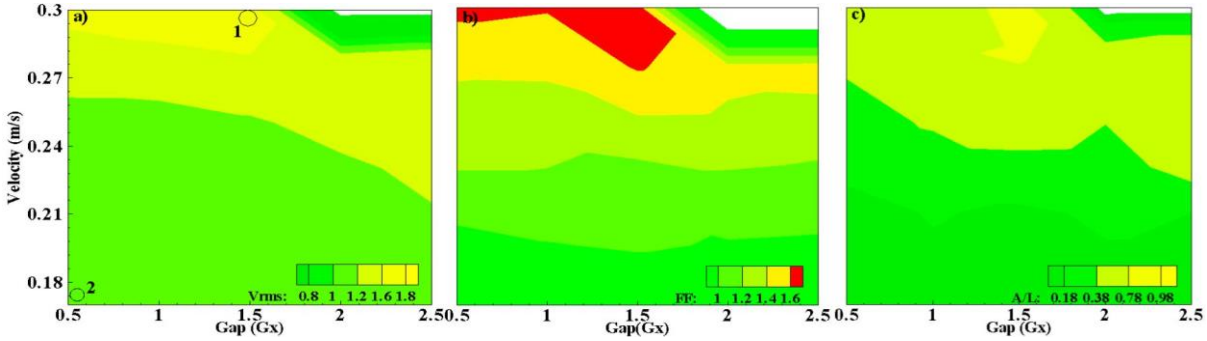


**Figure 13** Surface plots of a)Voltages generated " $V_{rms}$", b) flapping frequency and c)Amplitude "A/L" of the rear flag

As the flow velocity increased, root mean square voltages "$V_{rms}$", flapping frequency and the peak to peak amplitude "A/L" increased as shown in figures 13a, b and c respectively. Point 1 represents the maximum $V_{rms}$ of the rear flag at stream wise "Gx/L=1.5" and flow velocity V=0.3 m/s. As the dominant frequency of the flapping increased to the maximum of 1.697 Hz and peak to peak amplitude of the flag 0.9, Vrms got maximum. Point 2 shows the minimum value of $V_{rms}$ at a stream

wise gap and velocity of 0.5 and 0.17 m/s respectively. The rear flag was closed to the upstream flag, the fluid dynamic pressure exerted on the rear flag was less which resulted in lesser flapping frequency and peak to peak amplitude.

Yellow region in the surface plot represents the transition from low values to the higher values of the parameters. As shown in surface plot, at a velocity of 0.27 m/s values of voltages $V_{rms}$ remained within a close range of 1.3~1.5 at any stream wise gap Gx/L. At maximum velocity V=0.3 m/s rear flag got deflected at Gx/L= 2~2.5. This region is represented by white color in figures 13a, b and c.

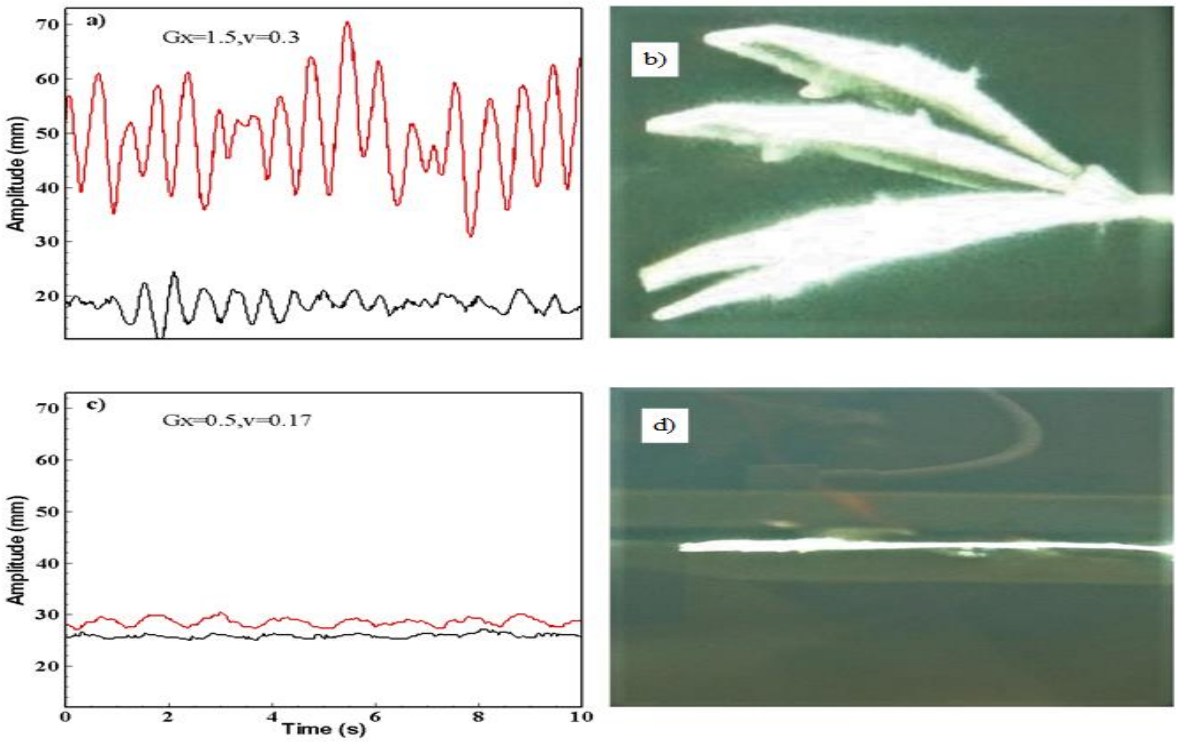


**Figure 14** (a) and (c) Amplitude curves (in mm) of rear flag (Red curve) and front flag (Black curve) at a gap and velocity of maximum and minimum voltage produced respectively. (b) and (d) Envelopes of the rear flag at that gaps and velocities.

Figures 14a and c represents the tail position of the front and rear flag at stream wise gaps of 1.5 and 0.5 respectively. The red and black curves represent the amplitude curves of the downstream and upstream flags respectively. The video has been recorded for 2 minutes and 10 seconds data has been presented here. The maximum amplitude traced "A/L" of the rear flag approached to 0.92 beyond which the flag got deflected. No match between peak to peak amplitudes of both the flags can be observed. Also it can be clearly seen in figures 14a and c that the curves are not regular and have non uniform fluctuations which occurs to be beat phenomenon. Also the frequency curves of both the flags are not in phase. The effect of inverted phenomenon is significant as the rear flag flapped with greater peak to peak amplitude as shown in figures. Envelopes of the rear flag at maximum and minimum values of the voltages are represented in figures 14 b and d respectively.

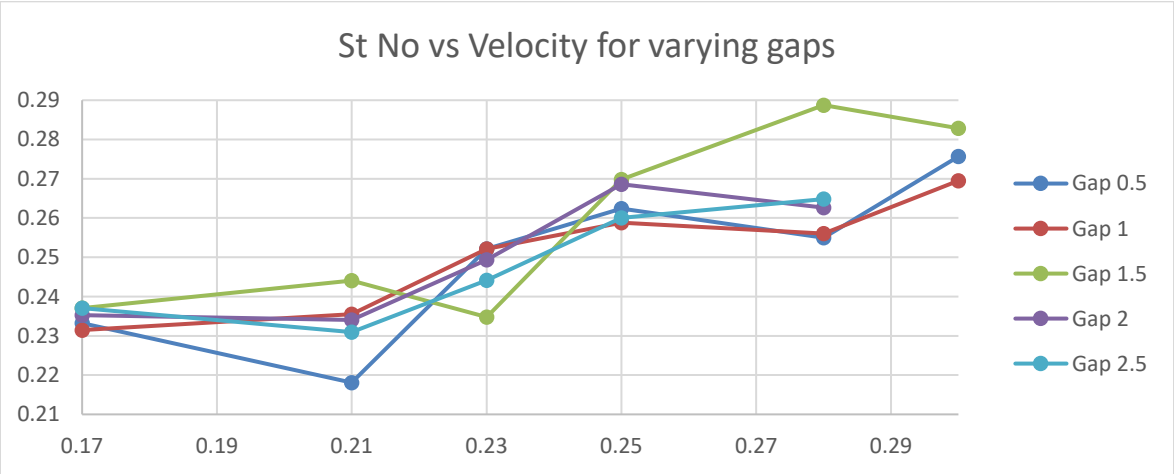


**Figure 15** Strouhal Number vs Flow Velocities plot for different stream wise gaps "Gx/L"

Figure 15 represents the plot for Strouhal number and flow velocities for varying stream wise gaps "Gx/L". The number ranged between 0.21 and 0.29 for all the gaps and velocities. The maximum and

minimum values of the Strouhal number corresponds well to that of the three chosen parameters i.e. $V_{rms}$ generated, flapping frequency and peak to peak amplitude "A/L". At Gx/L=1.5 Strouhal number increased to the maximum of 0.288 while at Gx/L=0.5 it decreased to the lowest.

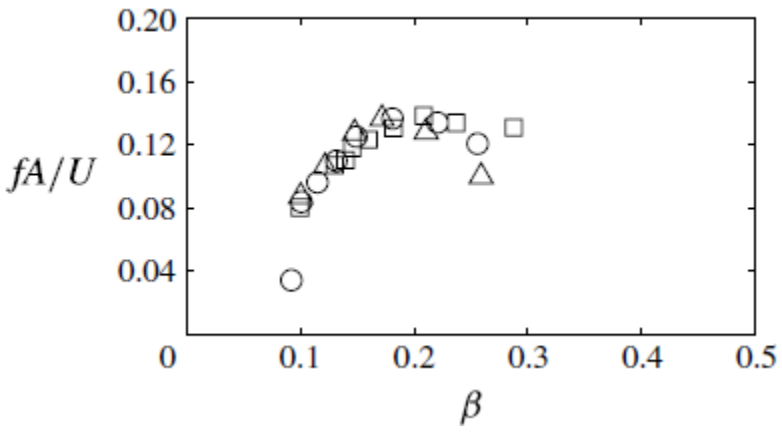


**Figure 16** Strouhal Number as a function of bending stiffness for mass ratio of 0 (1)[22]

Figure 16 represents the Stouhal number for a single inverted flag investigated experimentally by Kim [22]. By comparing the maximum Strouhal numbers obtained by both the flags (i.e. single inverted flag and the rear flag of our case), 42% increase of a Stouhal number can be seen which leads to the fact that relation between the flow velocity and flapping frequency of the rear flag is stronger than that of a single inverted flag. So a downstream flag in a tandem arrangement will flap more within a second than that of a single inverted flag at a single flow velocity.

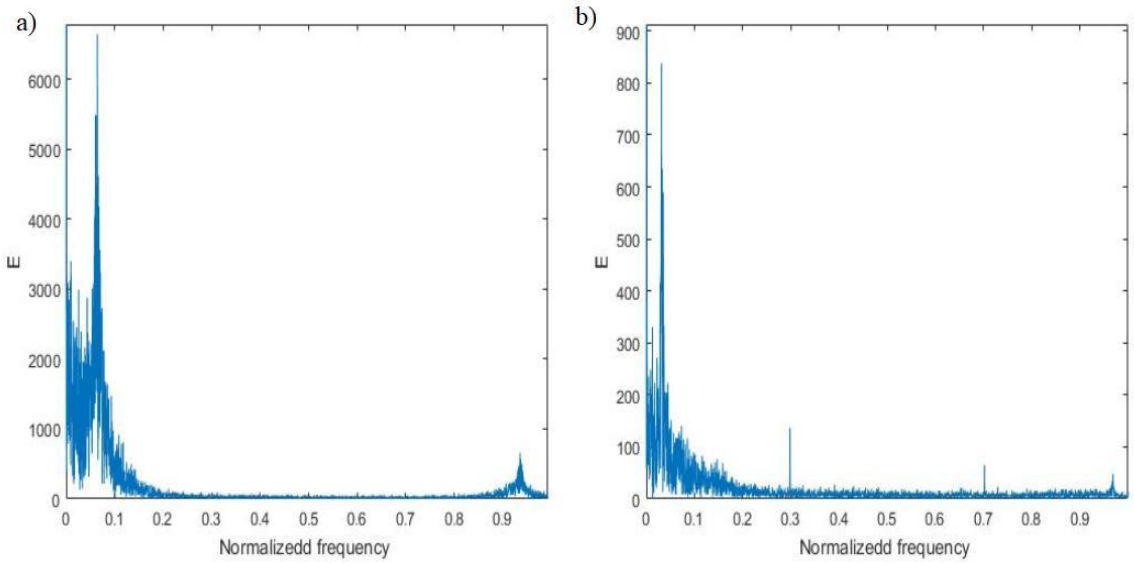


**Figure 17** Energy density plot for stream wise gaps and velocities of a) 1.5 & 0.3 m/s and b)0.5 & 0.17 m/s

Figures 17a and b represents the energy density spectrums for the stream wise gap and velocity of maximum and minimum voltages produced respectively. It is shown that the maximum energy acquired is almost 6 times of the minimum one and had reached to the peak value of 6000. The frequency of the signal was normalized to Nyquist frequency.

### 5.1.1. Case 1 (Flexural Rigidity=0.001 N.m) Average Values of the Peak to Peak Amplitudes

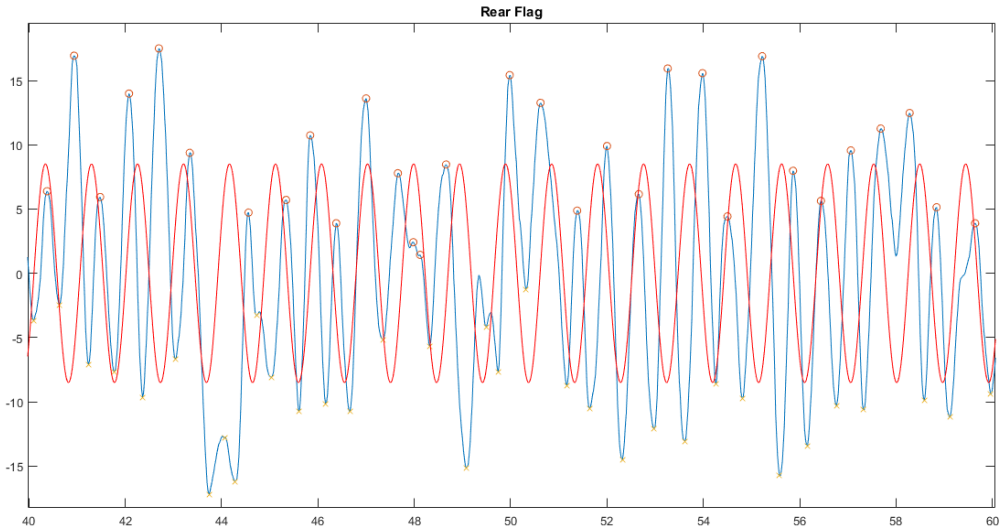


**Figure** 18 Average peak to peak amplitude of the Rear Flag

We also found the average values of the amplitude for each case (i.e. flexural rigidity "$\gamma$"=0.001,0.0015 and 0.002). The average peak to peak amplitude of the rear flag came out to 17.03 mm with a maximum value of 8.43 mm to one side of the mean position. The minimum value of flapping amplitude came out to be -8.60 mm to the other side of the mean position as shown in figure 18. Data here is presented for 20 seconds where blue and red curves are representing real and averaged curve of the peak to peak amplitude. Average value of flapping amplitude can now be used in expecting the average power extraction of the flag. The upper peak of the real amplitude deviated 4.49 mm from the mean position while the lower peak standard deviation from the mean position came out to be 4.21 mm.

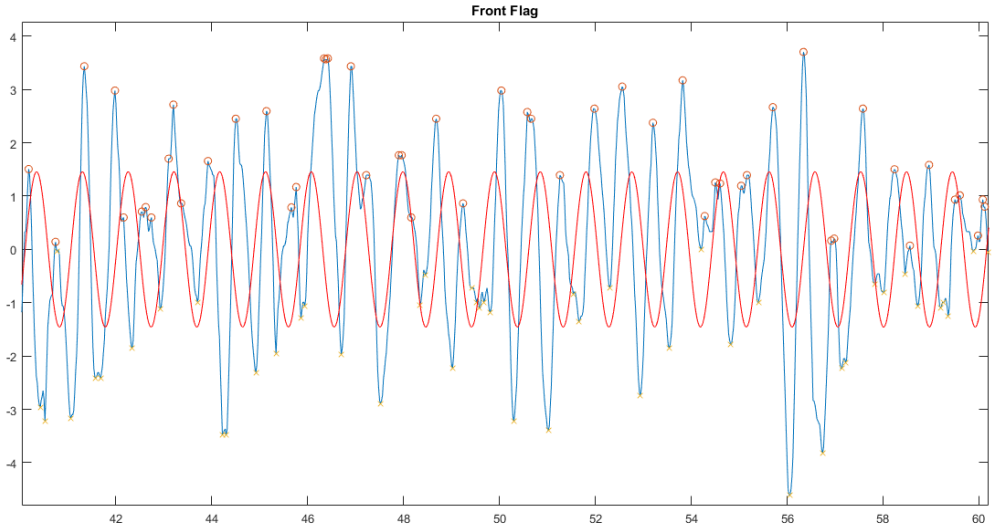


**Figure 19** Average peak to peak amplitude of the Front Flag

For the upstream flag, the average peak to peak value of flapping amplitude came out to be 2.91 mm with an upper peak of 1.37 mm. The average minimum value of flapping amplitude came out to be -1.54 mm. In both the cases of front and rear, the flag has flapped more towards the negative extreme than towards the positive extreme from the mean position. The upper peak of front flag deviated 0.98 mm from the mean position while the standard deviation of the lower peak is 1.15 mm. Figure 19 shows the upper and lower peaks of the real signal along with average peak to peak amplitude of the upstream flag.

## 5.2. Case 2 "Maximum Values" (Flexural Rigidity=0.0015 N.m)

In this case flexural rigidity of both the piezoelectric flags was increased to 0.0015 N.m by adding a laminated sheet of 60µm thickness to one side of both of them. The flags became stiffer and made them to flap lesser within a second than the previous case. At a gap and velocity of 1.5 and 0.3 m/s respectively, the rear flag flapped with the maximum frequency of 1.63 Hz as shown in figure 20 b. This led to maximum deformation of crystal lattice on the surface of the flexible body, which resulted in maximum $V_{rms}$ generated at the very gap and velocity as represented as point 1 in figure 20 a. However, no significant change in peak to peak amplitude was observed than that of the previous case. It also approached the value of 0.9 at a Gx/L=1.5 and V=0.3 m/s as shown in figure 20 c.

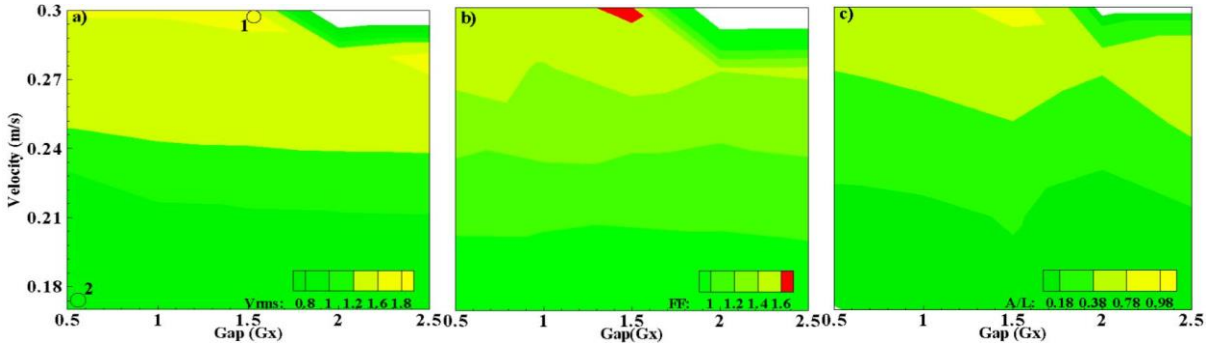


**Figure 20** Surface plots of a)Voltages generated " $V_{rms}$", b) flapping frequency and c)Amplitude "A/L" of the rear flag

The impact of varying velocity was also observed as can be seen the surface plots of all three parameters. Increase of velocity increased them to a certain level after which the flag deflected. That level came as the velocity approaches 0.3 at Gx/L=2~2.5. White regions in all three figures represent that region.

Below the stream wise gap of 1, at each velocity there was lesser peak to peak amplitude A/L observed as can be clearly seen in figure 20 b. This led to the possible occurrence of destructive mode of interaction of vortices downstream of the front flag. Point 2 in figure 20 a represents that stream wise gap of the lowest $V_{rms}$ generation. At this very gap and flow velocity, flapping frequency and the peak to peak amplitude of the downstream flag also had the lowest value. However, a gradual increase of A/L of the rear flag with the increase of flow velocity at each stream wise gap can be seen in figure 20 c.

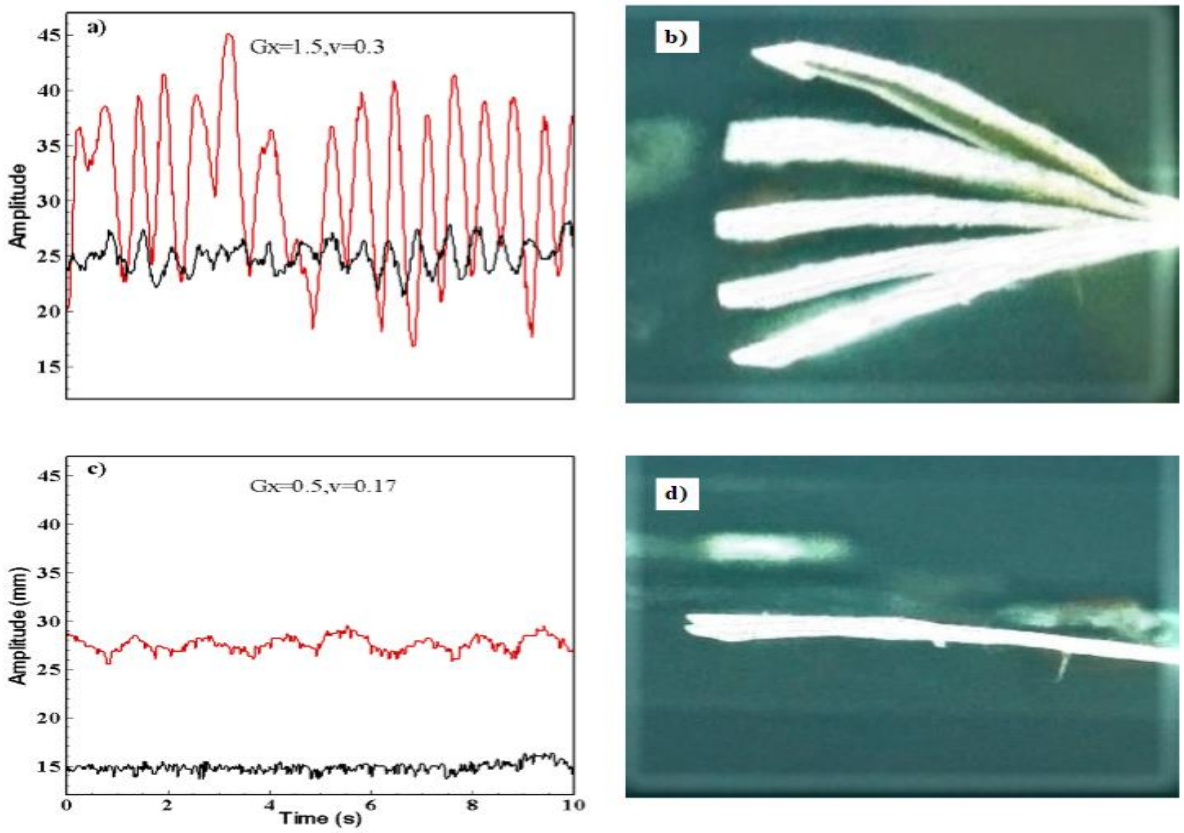


**Figure 21** a) and (c) Amplitude curves (in mm) of rear flag (Red curve) and front flag (Black curve) at a gap and velocity of maximum and minimum voltage produced respectively. (b) and (d) Envelopes of the rear flag at that gaps and velocities.

Figures 21a and c represents the tail position of the front and rear flag at stream wise gaps Gx/L of 1.5 and 0.5 respectively. Peak to peak amplitude of the rear flag is represented by red curve while the black curve represents the amplitude curve for the front flag. Video of the flapping flags was recorded for 120 seconds but only 10 seconds data has been shown in both the figures. The amplitude of the rear flag is almost 5 time of the amplitude of the upstream flag with no match of flapping frequencies. Beat phenomenon can be observed clearly as there is not any uniformity and the signals are fluctuating. Also it can be seen that both the flags (i.e. upstream and downstream) are not in phase in both maximum and minimum flapping case. The effect of inverted phenomenon is

significant as the rear flag flapped with greater peak to peak amplitude as shown in figures. Envelopes of the rear flag at maximum and minimum values of the voltages are represented in figures 21 b and d respectively.

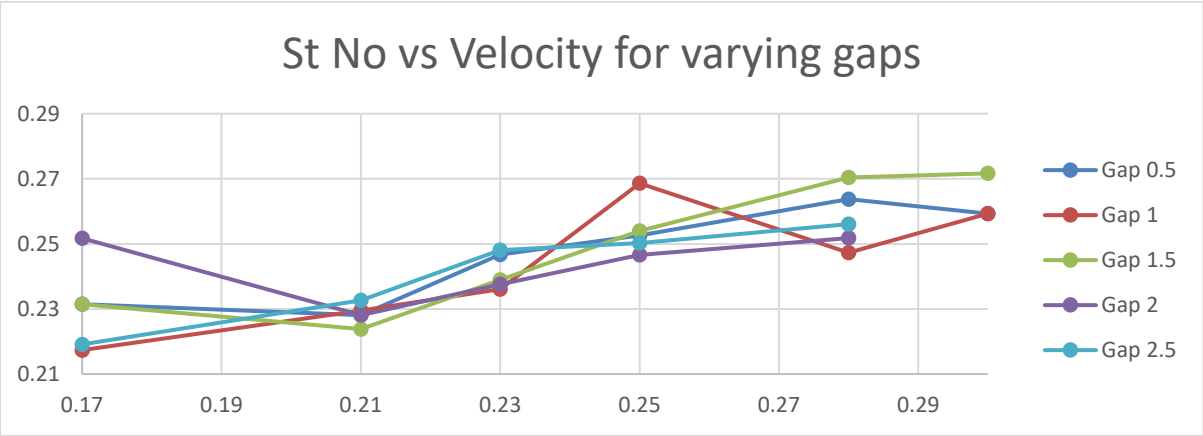


**Figure 22** Strouhal Number vs Flow Velocities plot for different stream wise gaps "Gx/L"

The graph between the Strouhal number and varying flow velocity for different stream wise gaps Gx/L has been shown in figure 22. In this case the number ranged between 0.21 and 0.27. Comparatively it dropped to the maximum of 0.271 than the previous case. However, it occurred exactly at the same stream wise gap where the other parameters had maximum values. At Gx/L=0.5 Strouhal number dropped to the minimum which also corresponds well to that of $V_{rms}$ produced, peak to peak amplitude and flapping frequency. Comparatively the increase in Strouhal number is 39 % of the single inverted flag (figure 16) which is lesser than the previous case (i.e. flexural rigidity= 0.001 N.m). This leads to the fact that in tandem arrangement the downstream flag will flap with greater frequency comparatively of an inverted flag at a constant flow velocity.

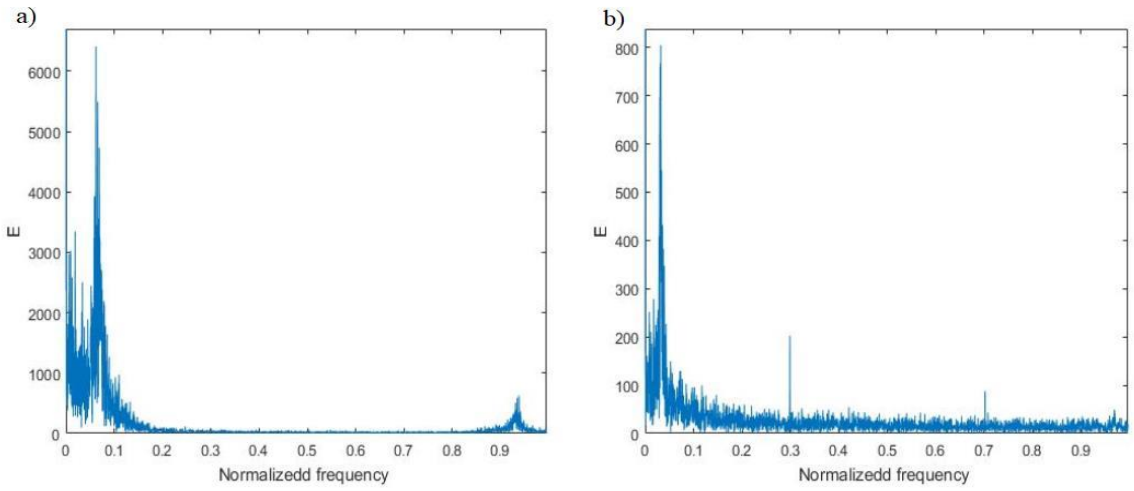


**Figure 23** Energy density plot for stream wise gaps and velocities of a) 1.5 & 0.3 m/s and b)0.5 & 0.17 m/s

Figures 23 a and b represents the energy density spectrums for the stream wise gap and velocity of maximum and minimum voltages produced respectively. A clear drop of energy density spectrum can be seen than that of the previous case. However, the ratio of the energy density of the maximum and minimum $V_{rms}$ remained more than 6 times. The frequency of the signal was normalized to Nyquist frequency.

### 5.2.1. Case 2 (Flexural Rigidity=0.0015 N.m) Average Values of the Peak to Peak Amplitudes

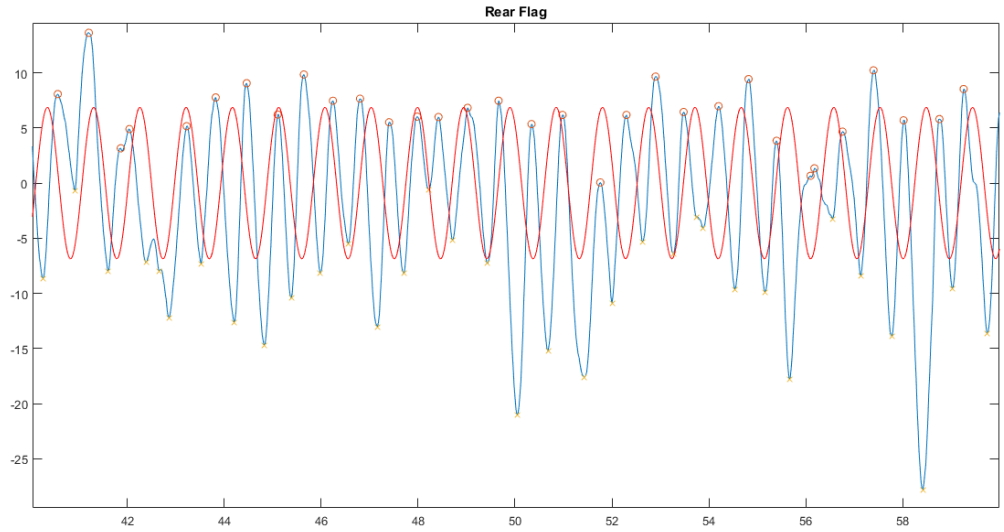


**Figure 24** Average peak to peak amplitude of the Rear Flag

In this case the average peak to peak amplitude of the rear flag dropped to 13.73 mm. The maximum amplitude traced by the flag came out to be 6.38 mm. The minimum value of flapping amplitude was -7.35 mm to the other side of the mean position as shown in figure 24. Data here is presented for 20 seconds where blue and red curves are representing real and averaged curve of the peak to peak amplitude. Average value of flapping amplitude can now be used in expecting the average power extraction of the flag. The upper peak of the real amplitude deviated 3.00 mm from the mean position while the lower peak standard deviation from the mean position came out to be 4.85 mm.

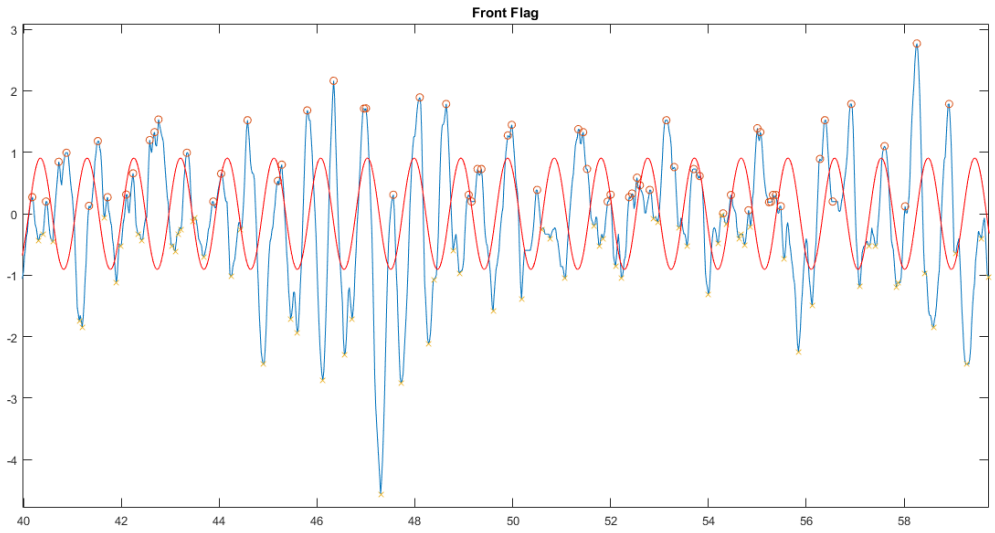


**Figure 25** Average peak to peak amplitude of the Front Flag

For the upstream flag, the average peak to peak value of flapping amplitude came out to be 1.81 mm with an upper peak of 0.89 mm. The average minimum value of flapping amplitude came out to be -0.91 0mm. In both the cases of front and rear, the flag has flapped more towards the negative extreme than towards the positive extreme from the mean position. The upper peak of front flag deviated 0.62 mm from the mean position while the standard deviation of the lower peak is 0.73 mm. Figure 25 shows the upper and lower peaks of the real signal along with average peak to peak amplitude of the upstream flag.

## 5.3. Case 3 "Maximum Values" (Flexural Rigidity=0.002 N.m)

In this case laminated sheet of 60µm was added to the other sides too of both the flags which increased the rigidity of the flags to 0.002 N.m. This increase of rigidity negatively affected the performance of the rear flag. Maximum root mean square voltages "$V_{rms}$" and flapping frequency of the rear flag dropped to 1.55 V and 1.367 Hz respectively as shown in figure 26 a and b. Point 1 in figure 26 a represents that stream wise gap Gx/L and flow velocity where voltages generation are maximum. Also maximum peak to peak amplitude "A/L" of the rear flag dropped to 0.8 which resulted in less deformation of crystal lattice on the surface of flag

as shown in figure 26 c. Lesser the deformation of lattice resulted in lesser $V_{rms}$ generation compartively to the above two cases. Minimum values of the parameters occurred at Gx/L=0.5 and v=0.17 m/s same as happened in case 1 and 2. This point is repesented as 2 in figure 26 a.

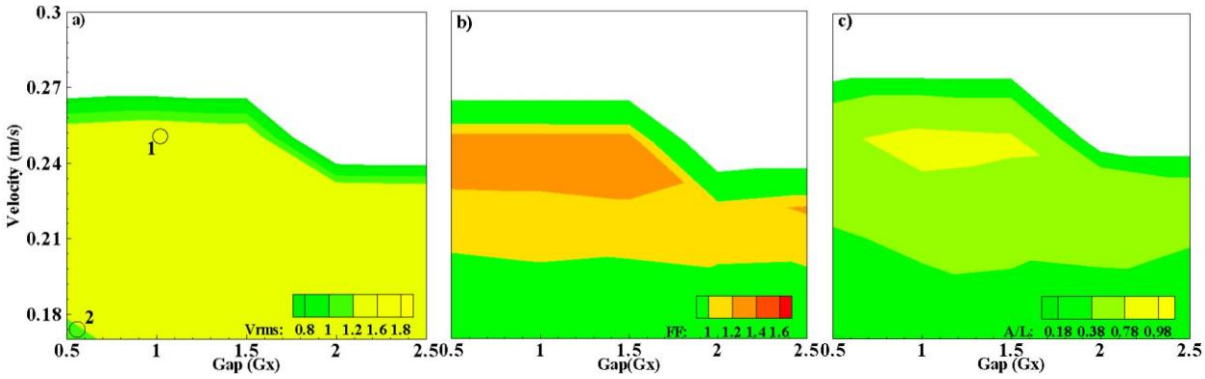


**Figure 26** Surface plots of a)Voltages generated " $V_{rms}$", b) flapping frequency and c)Amplitude "A/L" of the rear flag

Flow speed had also impacted the parameters in a positive way. Increasing the velocity of the flow increased the flapping frequency and A/L of the rear flag as shown in figures 26 b and c. However, change in $V_{rms}$ with respect to the flow was negligible in this case. It remained between a close range of 1.2 and 1.8 V. Maximum voltages were produced at Gx/L=1.5 and v=.025 m/s. Further increase of flow velocity made the rear flag to deflect at this very gap. At higher Gx/L of 2 and 2.5, the rear flag deflected even earlier which resulted in termination of flapping frequency of the flag. The deflected region is represented in white color in all three figures.

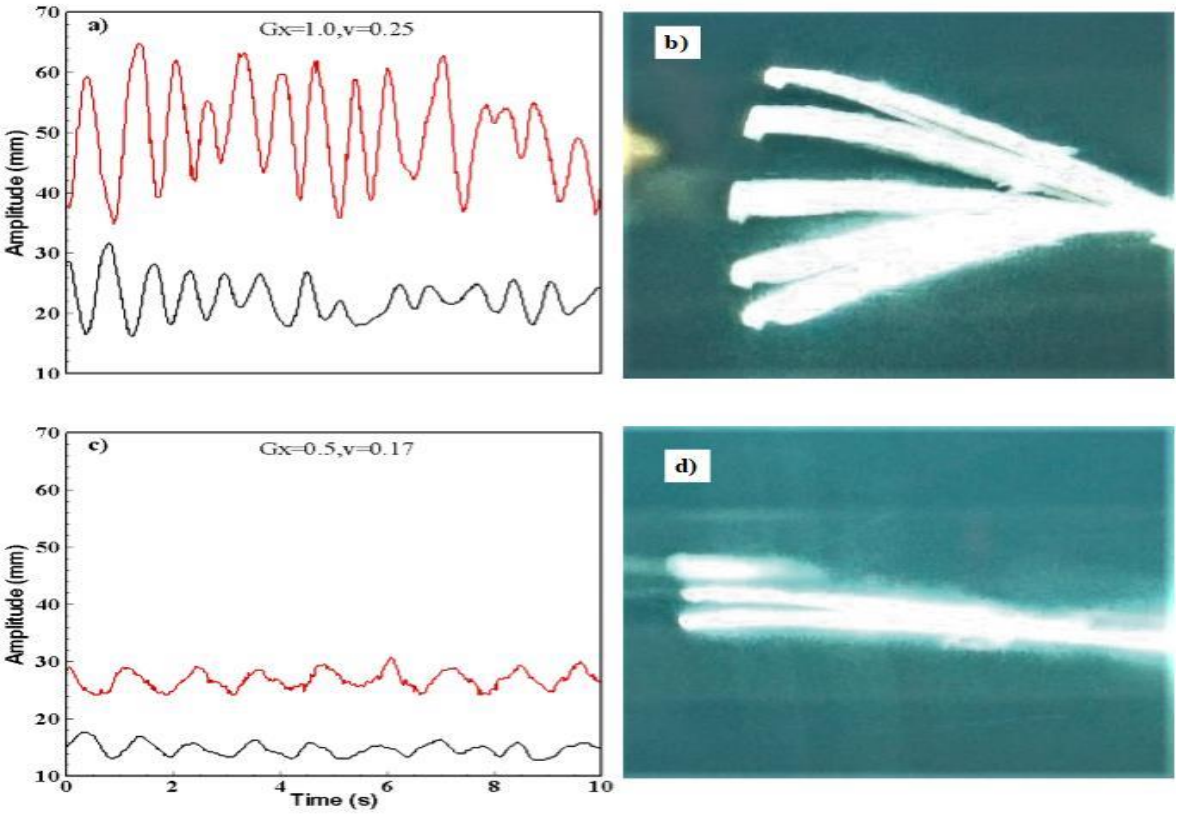


**Figure 27** (a) and (c) Amplitude curves (in mm) of rear flag (Red curve) and front flag (Black curve) at a gap and velocity of maximum and minimum voltage produced respectively. (b) and (d) Envelopes of the rear flag at that gaps and velocities.

Figures 27 a and c represents the tail position of the front and rear flag at stream wise gaps of 1 and 0.5 respectively. The red and black curves represent the amplitude curves of the downstream and upstream flags respectively. Video of the flapping flags has been recorded for 120 seconds but only 10 seconds data is presented here. There is not any uniformity and the signals of both the flags are fluctuating. The curves of both the flags have opposite sides of peak (i.e. crest of the downstream flag are meeting troughs of the upstream flag). Also both the signals are not synchronizing which leads to the fact that both the flags (i.e. upstream and downstream) flaps with different flapping frequencies. This difference of frequencies of both the flags can also be seen at the lowest values of the

parameters (i.e. Gx/L=0.5 and v=0.3m/s). The effect of inverted phenomenon is significant as the rear flag flapped with greater peak to peak amplitude as shown in figures. This leads to the fact that the drag on the downstream flag is greater than that on the upstream flag. Envelopes of the rear flag at maximum and minimum values of the voltages are represented in figures 27 b and d respectively.

.

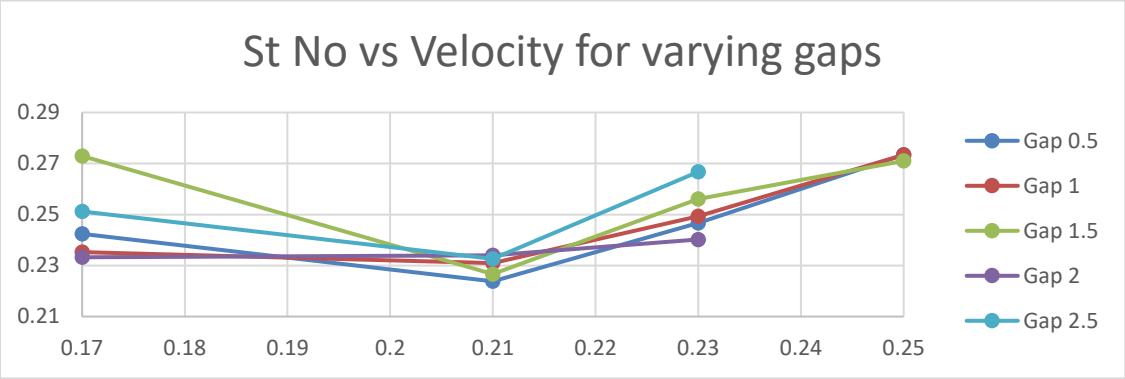


**Figure 28** Strouhal Number vs Flow Velocities plot for different stream wise gaps "Gx/L"

Figure 28 represents the plot for Strouhal number and flow velocities for varying stream wise gaps "Gx/L". The number ranged between 0.21 and 0.27 for all the gaps and velocities. The maximum and minimum values of the Strouhal number corresponds well to that of the three chosen parameters i.e. $V_{rms}$ generated, flapping frequency and amplitude traced "A/L". In comparison with the maximum Stouhal number achieved in an inverted flag configuration (figure 16), it increases almost 39%. However, there is not any significant change in Strouhal number as the rigidity has been increased. At Gx/L=1.0 Strouhal number increased to the maximum of 0.27 and decreased to 0.21 at stream wise gap of Gx/L=2.0.

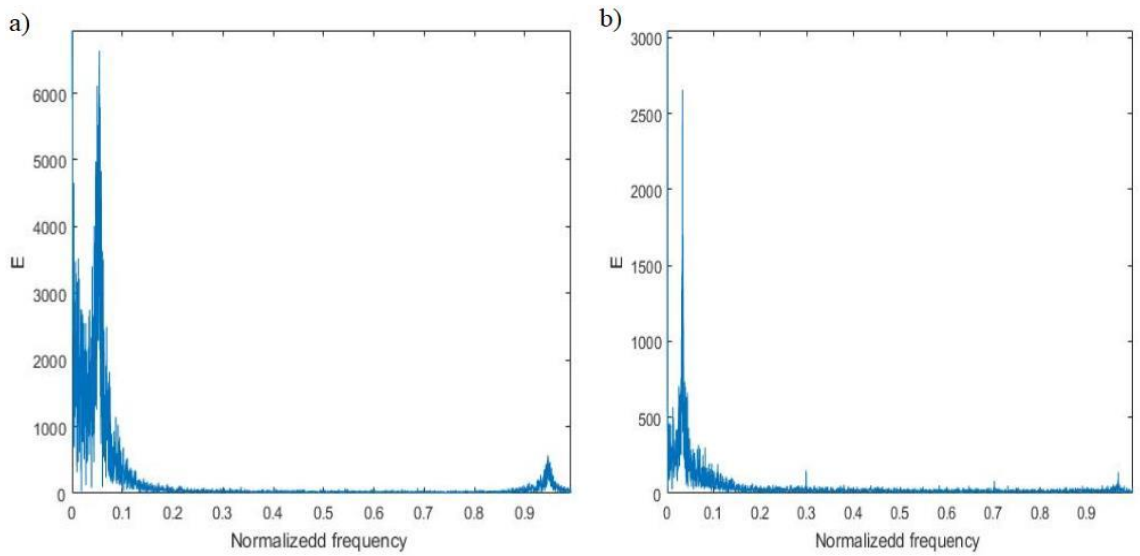


**Figure 29** Energy density plot for stream wise gaps and velocities of a) 1.5 & 0.3 m/s and b)0.5 & 0.17 m/s

Figures 29 a and b represents the energy density spectrums for the stream wise gap and velocity of maximum and minimum voltages produced respectively. In this case the minimum achieved energy density has exceeded 2500 while the spectrum for the maximum $V_{rms}$ is still in that range of above 6000. So the difference between the maximum and minimum value decreased almost 2 times. The frequency of the signal was normalized to Nyquist frequency.

### 5.3.1. Case 3 (Flexural Rigidity=0.002 N.m) Average Values of the Peak to Peak Amplitudes

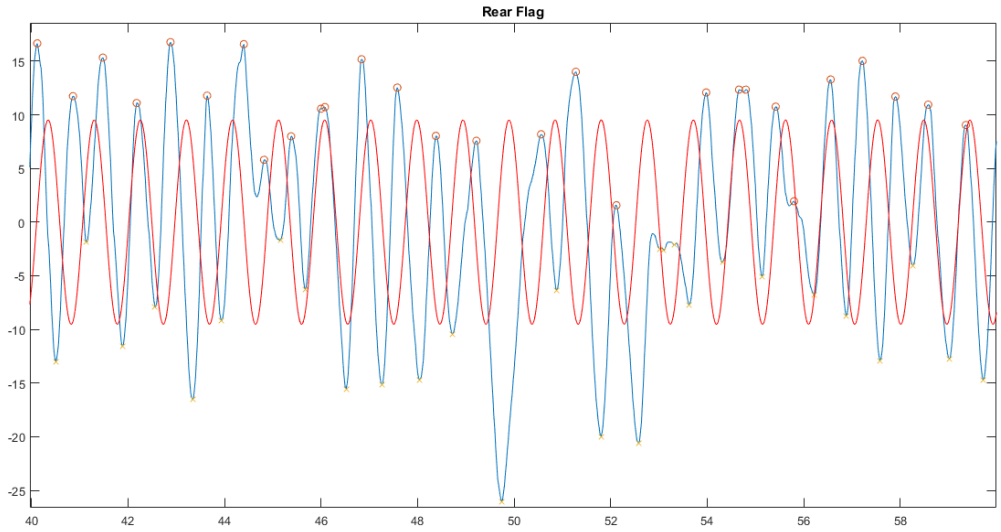


**Figure 30** Average peak to peak amplitude of the Rear Flag

In this case the average peak to peak amplitude of the rear flag came out to 19.05 mm with a maximum value of 9.87 mm to one side of the mean position. The minimum value of flapping amplitude came out to be -9.17 mm to the other side of the mean position as shown in figure 30. Data here is presented for 20 seconds where blue and red curves are representing real and averaged curve of the peak to peak amplitude. Average value of flapping amplitude can now be used in expecting the average power extraction of the flag. The upper peak of the real amplitude deviated 4.82 mm from the mean position while the lower peak standard deviation from the mean position came out to be 6.10 mm.

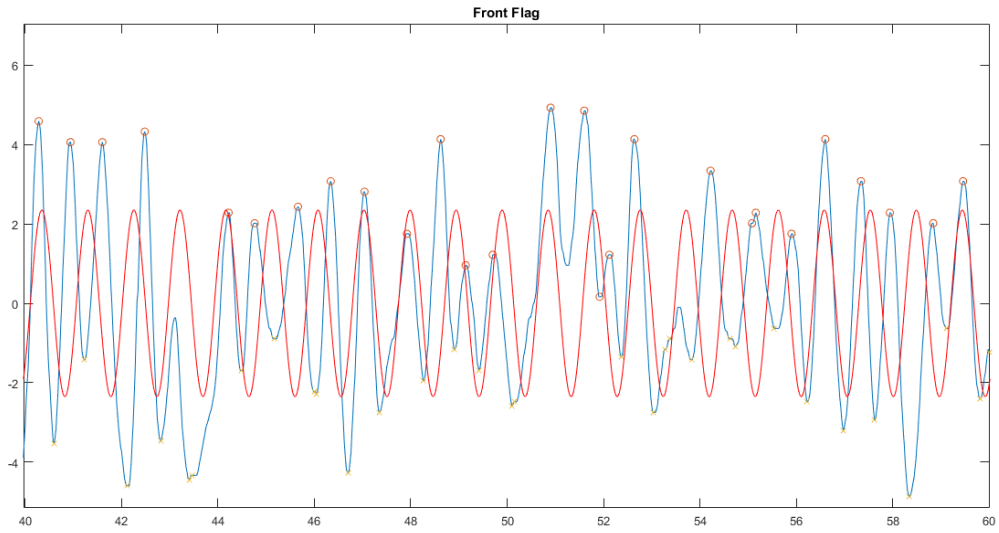


**Figure 31** Average peak to peak amplitude of the Front Flag

For the upstream flag, the average peak to peak value of flapping amplitude came out to be 4.70 mm with an upper peak of 2.47 mm. The average minimum value of flapping amplitude came out to be -2.22 mm. The upper peak of front flag deviated 1.70 mm from the mean position while the standard deviation of the lower peak is 1.47 mm. Figure 31 shows the upper and lower peaks of the real signal along with average peak to peak amplitude of the upstream flag.

# Conclusion

In the present study, performance of the tandem arrangement of two inverted flags in a water tunnel has been investigated. Effects of varying flexural rigidity, stream wise gaps between them and flow velocity on voltages generated, flapping frequency and A/L of the downstream flag have been analyzed. Upstream flag was not considered for the study purpose due to the inverted drafting phenomenon. However, amplitudes of both the flags were compared at maximum and minimum values of voltages generated. Increasing the rigidity negatively affected the flapping frequency and voltages generation of the rear flag. This resulted in optimum values at $\gamma$ =0.001 N.m. However, A/L was not affected much by it. We got maximum voltages along with the flapping frequency at Gx/L=1.5 and v=0.3 m/s. Furthermore, it has been observed that the downstream flag flapped with greater amplitude than that of front flag due to the greater drag on rear one. This phenomenon is known as inverted drafting which occurs in flexible bodies only. Rear flag showed deflection even at very low flapping of the front one which limited the increase of velocity of the flow. This experimentation suggested that the range of velocity and stream wise gap should be kept small with small steps which will enable the researcher to avoid the earlier deflection and getting precise gap and flow velocity optimization.

# REFERENCES


[1] Tofa. ; 2012 “Fundamentals of vortex induced vibration analysis of marine riser” ; The 6th Asia-Pacific Workshop on Marine Hydrodynamics (APHydro2012)

[2] Nishioka. ; 1978 “ Mechanism of determination of the shedding frequency of vortices behind a cylinder at low Reynolds numbers” ; J. Fluid Mech. (1978), vol. 89, part 1,pp. 49-60

[3] Huerre. ; 1990 “Local and global instabilities in spatially developing flows” ; Annu. Rev. Fluid Mech. 1990.22: 473-537

[4] Friehe. ; 1980 “Vortex shedding from cylinders at low Reynolds numbers” ; J. Fluid Mech. (1980), vol. 100, part 2, pp. 237-241

[5] Roshko ; 1954 “On the development of turbulent wakes from vortex streets” ; Calfornia University of Technology, USA

[6] Roshko ; 1961 “Experiments on the flow past a circular cylinder at very high Reynolds number” ; Calfornia University of Technology, USA

[7] Nickerson ; 1981 “On the existence of atmospheric vortices downhill of Hawaii during the HAMEC project” ; Journal of applied meteorology

[8] Torum ; 1985 “Free span vibrations of submarine pipelines in steady flows-effect of free-stream turbulence on mean drag coefficients” Journal in Energy Resources Technology

[9] Tsahalis ; 1984“Vortex-Induced Vibrations of a Flexible Cylinder Near a Plane Boundary Exposed to Steady and Wave-Induced Currents” ; Journal of Energy Resources Technology, Transactions of the ASME 106(2):206-213

[10] Bearman ; 1978 “Flow around a circular cylinder near a plane boundary” ; Journal of Fluid Mechanics 89(01):33 – 47

[11] Buresti ; 1979 “Vortex Shedding from Smooth and Roughened Cylinders in Cross-Flow near a Plane Surface” ; Aeronautical Quarterly 30(01):305-321 · February 1979

[12] Kiya ; 1980 “Vortex shedding from two circular cylinders in staggered arrangement” ; ASME J. Fluids Eng., 102,pp. 166-171

[13] Sarpkaya ; 1979 “Vortex-Induced Oscillations: A Selective Review” ; *J. Appl. Mech* 46(2), 241-258 (Jun 01, 1979)

[14] Griffin ; 1975 “Vortex shedding from a cylinder vibrating in line with an incident uniform flow” ; J. Fluid Mech. (1976), vol. 75, part 2, pp. 257-271

[15] Bishop ; 1964 “The lift and drag forces on a circular cylinder oscillating in a flowing fluid” ; Department of Mechanical Engineering, University College London

[16] Stansby ; 1976 “The locking-on of vortex shedding due to the cross-stream vibration of circular cylinders in uniform and shear flows” ; Journal of Fluid Mechanics, vol. 74, Apr. 22, 1976, p. 641-665.

[17] Williamson ; 1988 “Vortex formation in the wake of an oscillating cylinder” ; Journal of Fluids and Structures (1988) 2, 355-381

[18] Blevins ; 1999 “Flow Induced Vibrations” Chap 3;3.3

[19] Bearman ; 1982 “An experimental study of pressure fluctuations on fixed and oscillating square-section cylinders” ; J. Fluid Mech. (1982), vol. 119, pp. 297-321

[20] Teimourian ; 2018 “Vortex Shedding: A Review on Flat Plat” ; ISSN 0015-4628, Fluid Dynamics, 2018, Vol. 53, No. 2, pp. 212–221

[22] Kim ; 2013 “Flapping dynamics of an inverted flag” ; J. Fluid Mech. (2013), vol. 736, R1

[23] Orrego ; 2017 “Harvesting ambient wind energy with an inverted piezoelectric flag” ; Applied Energy 194 (2017) 212–222

[24] Kim ; 2010 “ Constructive and destructive interaction modes between two tandem flexible flags in viscous flow” ; J. Fluid Mech. (2010), vol. 661, pp. 511–521

[25] Mazharmanesh ; 2018 “Energy Harvesting of Two Inverted Piezoelectric Flags in Tandem Arrangement” ; 21st Australasian Fluid Mechanics Conference

[26] Choi ; 1998 “Wind tunnel blockage effects on aerodynamic behavior of bluff body” ; Wind and Structures, Vol. 1, No. 4 (1998) 351-364

[27] Huang ; 2017 “Coupling performance of tandem flexible inverted flags in a uniform flow” ; J. Fluid Mech. (2018), vol. 837, pp. 461_476.

[28] Ristoph ; 2008 "Anomalous Hydrodynamic Drafting of Interacting Flapping Flags” PRL 101, 194502 (2008) PHYSICAL REVIEW LETTERS

[29] J. Zhang ; 2000 “Flexible filaments in a flowing soap film as a model for one-dimensional flags in a two-dimensional wind,” Nature, vol. 408, pp. 835–839.

[30] Lienhard ; 1966 “Synopsis of lift, drag and vortex frequency data for rigid circular cylinders.

# CERTIFICATE OF COMPLETENESS

It is hereby certified that the dissertation submitted by NS Danish Ahmad, Reg No. **00000171022**, Titled: ***Experimental investigation of tandem arrangement of two inverted flags in the wake of a cylinder*** has been checked/reviewed and its contents are complete in all respects.

Supervisor's Name: **Dr. Zafar Abbas Bangash** Signature: _____

Date: _____